



Flow and heat transfer in biological tissue due to electromagnetic near-field exposure effects



Teerapot Wessapan^a, Phadungsak Rattanadecho^{b,*}

^a School of Aviation, Eastern Asia University, Pathumthani 12110, Thailand

^b Center of Excellence in Electromagnetic Energy Utilization in Engineering (CEEE), Department of Mechanical Engineering, Faculty of Engineering, Thammasat University (Rangsit Campus), Pathumthani 12120, Thailand

ARTICLE INFO

Article history:

Received 20 August 2015

Received in revised form 8 February 2016

Accepted 9 February 2016

Keywords:

Electromagnetic fields

Porous media

Specific absorption rate

Biological tissue

Near-field

ABSTRACT

Electromagnetic fields (EMF) have been a vital part of our daily life over the past decade. Therefore, people are continuously exposed to electromagnetic (EM) sources in their vicinity generated by electronic devices such as those emitted by Wi-Fi, mobile phones, portable wireless router and other wireless services. This study aims to investigate the SAR, fluid flow and heat transfer in biological tissue due to EM near-field exposure. In a tissue model, the effects of distance to an EMF source and tissue permeability on natural convection in the biological tissue are systematically investigated. The specific absorption rate (SAR), fluid flow and the temperature distributions in the tissue during exposure to EM fields are obtained by numerical simulation of EM wave propagation and heat transfer equations. The EM wave propagation is expressed mathematically by Maxwell's equations. The heat transfer model used in this study is developed based on bioheat model and porous media model. By using the porous media model, the distribution patterns of temperature are quite different from the bioheat model by the strong blood dissipation effect of the porous media model. The exposure distance significantly influences the SAR, velocity field and temperature distribution. Moreover, the tissue permeability also affects the temperature distribution patterns within the tissue. The obtained results may be of assistance in determining exposure limits for the power output of the wireless transmitter, and its distance from the human body. The results can also be used as a guideline to clinical practitioners in EM relates the interaction of the radiated waves with the human body.

© 2016 Elsevier Ltd. All rights reserved.

1. Introduction

During recent years there has been increasing public concern on potential health risks from radiation emission from wireless communication systems. All wireless electronic devices generate electromagnetic field (EMF). EMF travel indefinitely through space and disturb other electromagnetic changes in their vicinity. The user of these electronic devices is exposed to electromagnetic (EM) radiation in the near field of the EM source. However, recommendations on EM exposure limits are specified in terms of the far-field parameters. The recommendations which limit the exposure have been issued by the International Commission on Non-Ionizing Radiation Protection (ICNIRP) [1] and the Institute of Electrical and Electronics Engineers (IEEE) [2]. Moreover, available study on the SAR, heat

transfer and fluid flow in biological tissues exposed in the near-field are very limited.

At microwave frequencies, the main biological effect of EM near-field exposure is heating. Most previous studies of the interaction between EMF and the biological tissue were mainly focused on SAR and have not been considered heat transfer and blood flow causing an incomplete analysis to the results. Actually, the severity of the physiological effect produced by small temperature increases can be expected to worsen in sensitive organs. An increase of approximately 1–5 °C in human body temperature can cause numerous malformations, temporary infertility in males, brain lesions, and blood chemistry changes. Even a small temperature increase in human body approximately 1 °C can lead to altered production of hormones and suppressed immune response [3]. Therefore, the realistic modeling of the complex phenomena associated with the heat transport is needed in order to completely explain the actual process of interaction between EM field and the biological tissue.

* Corresponding author.

E-mail addresses: teerapot@eau.ac.th (T. Wessapan), ratphadu@engr.tu.ac.th (P. Rattanadecho).

Nomenclature

C	specific heat capacity (J/(kg K))
E	electric field intensity (V/m)
f	frequency of incident wave (Hz)
H	magnetic field (A/m)
j	current density (A/m ²)
k	thermal conductivity (W/(m K))
n	normal vector
p	pressure (N/m ²)
Q	heat source (W/m ³)
T	temperature (K)
u	velocity (m/s)
t	time

Greek letters

β	volume expansion coefficient (1/K)
μ	magnetic permeability (H/m)
ε	permittivity (F/m)
ε_p	porosity

σ	electric conductivity (S/m)
ρ	density (kg/m ³)
ω	angular frequency (rad/s)
ω_b	blood perfusion rate (1/s)
μ	dynamic viscosity (N s/m ²)

Subscripts

b	blood
ext	external
eff	effective
met	metabolic
r	relative
s	solid
ref	reference
0	free space, initial condition

Recently, transport models of biological tissue have been rapidly developed and have been used extensively in studies of the health implications of exposure to EMF and prediction of therapeutic responses to EMF. The most widely used bioheat model was introduced by Pennes [4]. Due to simplifications of Pennes' bioheat model, other workers have established mathematical bioheat models by extending or modifying Pennes model [5–7]. Some bioheat models are also established and examined for countercurrent heat transfer in arterial–venous blood vessels [8,9]. Recently, there has been an increasing attention to using porous media in modeling flow and heat transfer in biological tissues [10–13,29]. The theory of porous media for heat transfer in biological tissues is found to be most appropriate since it contains fewer assumptions, are stressed by Khaled and Vafai [14], Nakayama and Kuwahara [15], and Khanafer and Vafai [16,13]. The volume averaging method has also been widely used to develop the transport equation for countercurrent bioheat transfer between terminal arteries and veins in the circulatory system [15]. Advances in modeling of transport process in biological tissue subjected to hyperthermia have been recently carried out [17,18].

Our research group has numerically investigated the temperature increase in human tissue subjected to EM fields in many problems [19–30]. Wessapan et al. [19,20] utilized a 2D finite element method (FEM) to obtain the specific absorption rate (SAR) and temperature increase in the human body exposed to leaked EM waves. Wessapan et al. [21,22] developed a 3D model of the human head in order to investigate the SAR and temperature distributions in the human head during exposure to mobile phone radiation. Wessapan et al. [23–26] investigated the SAR, fluid flow and temperature distributions in the eye during exposure to EM waves using porous media theory. Keangin et al. carried out a numerical simulation of liver cancer treated using a mathematical model that considered the coupled model of EM wave propagation, heat transfer, and mechanical deformation in the biological tissue in the couple's way [27]. They also include more advanced applications in the model such as the different types of antennas [28] and include the porous media effects into their model [29]. Keangin et al. proposed a model to investigate the effect of EMF on biological tissue using porous media theory based on thermal non-equilibrium (LTNE) model [30].

Although porous media involves natural convection in biological tissue have been used in the previous biomedical studies [29,30], most studies of biological tissue exposed to EMF have

not been considering the porous media approach especially in near-field problems. Therefore, the actual thermo-physiologic response of the biological tissues subject to a near-field EMF is still not well understood due to the physical complexity associated with transport in biological tissue and EMF propagation.

The present study utilizes the porous media theory to analyze SAR, fluid flow and heat transfer in biological tissue subjected to a near-field EMF. The dipole antenna is the most common design for omnidirectional antennas and is used as an EM source in this study. The EM wave propagation emitted from the antenna propagate through the tissue is expressed mathematically by Maxwell's equations. In the tissue model, the effects of distance to an EMF source and tissue permeability on natural convection in the biological tissue is systematically investigated. The SAR, fluid flow and temperature distributions in the tissue during exposure to EM fields are obtained by numerical simulation of the EM wave propagation and heat transfer equations. In particular, the results obtained from the porous media model, considered natural convection, are compared with the results obtained from a convective bioheat model. The exposure frequency of 900 MHz is selected because of it is frequently used in various industrial, medical and wireless transmitters. The obtained results may be of assistance in determining exposure limits for the power output of the wireless transmitter, and its distance from the human body. The results can also be used as a guideline to clinical practitioners in EM relates the interaction of the radiated waves with the human body.

2. Formulation of the problem

In general, total personal exposure consists of contributions from near-field and far-field sources with respect to the human body. These EM energy can lead to temperature rise produced in body tissue which can cause a number of adverse human health effects. Near-field sources such as mobile phones and portable wireless router operate in close vicinity of the body and can cause temporarily high local exposure. For adequate study of transport phenomena in the human tissue caused by EM near-field exposures, the contribution of different EM sources to the human exposure of different body tissues is required. Fig. 1 shows human exposure to near-field EM radiation.

This study investigates the effect of EM near-field exposure on SAR, fluid flow and heat transfer in biological tissue. Due to ethical

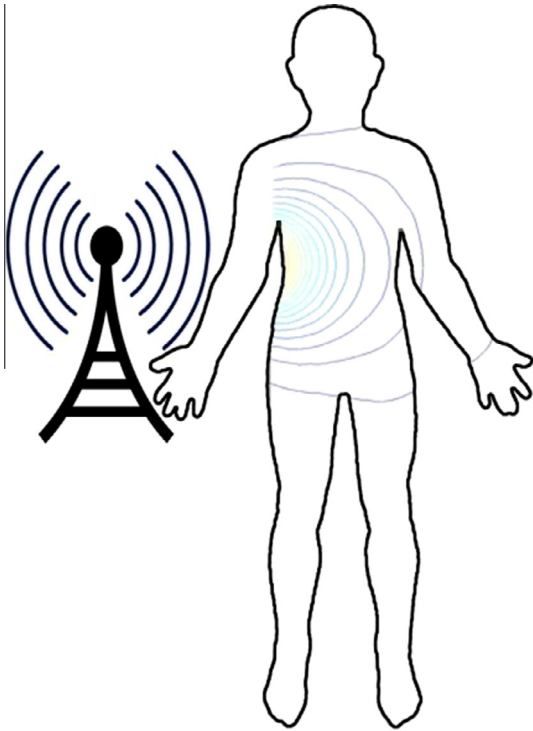


Fig. 1. Human exposure to near-field EM radiation.

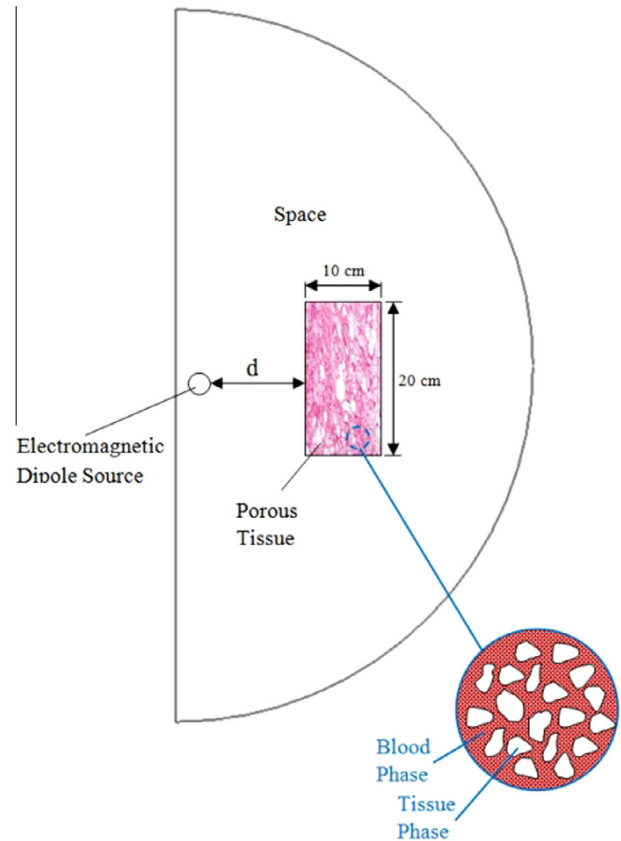


Fig. 2. The computational domain of the problem.

consideration, exposing the living human to EM fields for experimental purposes is limited. It is more convenient to develop a realistic biological tissue model, including transport processes through the numerical simulation. A highlight of this work is the illustration of the transport phenomena, including the heat transfer and fluid flow in the biological tissue during exposure to near-field EMF in different conditions. The SAR, fluid flow and heat transfer are numerically investigated in a tissue model from near-field exposure to a dipole source, operated at 900 MHz, will be illustrated in Section 3. The system of governing equations as well as the initial and boundary conditions are solved numerically using the finite element method (FEM).

3. Methods and model

The study focuses attention on the differences in heat transfer characteristics of the tissue induced by near-field EM radiation from a dipole antenna source. The first step in evaluating the effects of a certain exposure to EM fields in the tissue is to determine the induced internal EM fields and its spatial distribution. Thereafter, EM energy absorption which results in a temperature increase in the tissue and other process of transport phenomena will be considered. This study considers the heat transfer and transport consequences of such exposure and their implications for the threshold for EM hazard.

3.1. Physical model

Fig. 2 shows the computational domain of the problem, in which an interaction between the tissue and the dipole antenna take place. The tissue model considered in this study can be treated as a blood saturated tissue represented by a porous medium. The tissue model is divided into the vascular region (blood phase) and the extra-vascular region (tissue phase), as illustrated in Fig. 2. In this study, a 2D model is considered in order to minimize

the amount of computational time while maintain resolution. In order to investigate of the EM near-field exposure effects on biological tissue, a rectangular model of biological tissue with the length of 10 cm and height of 20 cm is exposed to an electric dipole antenna. The tissue model assumes that the tissue is regarded as a semi-infinite plane medium. The dipole is excited at the center feed point, the transmitted power is determined as the complex product of the current and voltage at the feed point. The dipole used operates at 900 MHz frequency and transmits the radiated power of 0.6 W, the approximate output of general mobile phone and wireless transmitters. The dipole source is placed at 4 different distances at $d = 0.5, 1.0, 3.0, 5.0$ cm from the tissue surface. Fig. 3 shows the computational domain used in this study. The tissue is assumed to be a homogeneous, electrically and thermally isotropic as well as saturated porous medium. There is no effect on the chemical reaction and phase change within the tissue.

3.2. Equations for EM wave propagation analysis

The mathematical models are developed to predict the EM fields and the SAR which corresponds to the temperature gradient in the tissue. To simplify the problem, the following assumptions are made:

1. The EM wave propagation is modeled in two dimensions.
2. The EM wave interact with the tissue proceeds in the open region.
3. The free space is truncated by scattering boundary condition.
4. The model assumes that dielectric properties of the porous tissue are uniform and constant.
5. The radiated waves from the dipole are characterized by transverse electric (TE) fields.

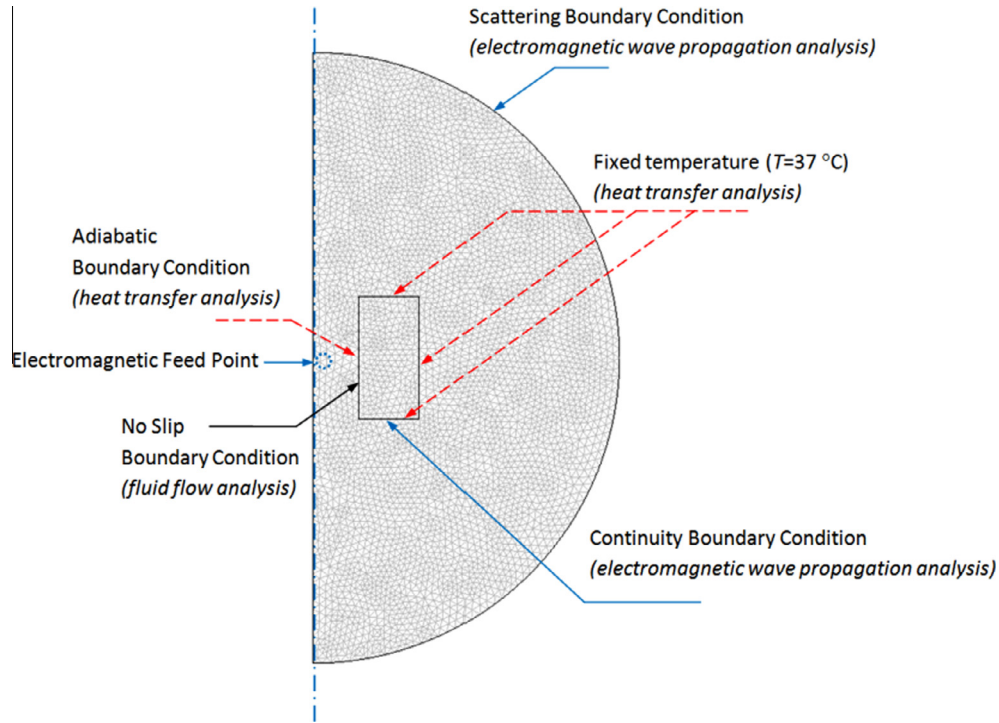


Fig. 3. Boundary condition for analysis of EM wave propagation, fluid flow and heat transfer.

The EM wave propagation is calculated using Maxwell's equations [19,31] which mathematically describe the interdependence of the EM waves. The general form of Maxwell's equations is simplified to demonstrate the EM field penetrated into the tissue as the following equation:

$$\nabla \times \left(\frac{1}{\mu_r} \nabla \times E \right) - k_0^2 \left(\epsilon_r - \frac{j\sigma}{\omega\epsilon_0} \right) E = 0 \quad (1)$$

$$\epsilon_r = n^2 \quad (2)$$

where E is electric field intensity (V/m), μ_r is relative magnetic permeability, n is refractive index, ϵ_r is relative dielectric constant, $\epsilon_0 = 8.8542 \times 10^{-12}$ F/m is permittivity of free space, σ is electric conductivity (S/m), $j = \sqrt{-1}$ and k_0 is the free space wave number (m^{-1}).

3.2.1. Boundary condition for wave propagation analysis

Boundary conditions along the interfaces between different mediums, namely, between air and tissue, are considered as continuity boundary condition,

$$n \times (H_1 - H_2) = 0 \quad (3)$$

The outer sides of the calculated domain, i.e., free space, are considered as scattering boundary condition to eliminate the reflections,

$$n \times (\nabla \times E) - jkE = 0 \quad (4)$$

where k is the wave number (m^{-1}), n is normal vector, $j = \sqrt{-1}$, and H is the magnetic field (A/m).

3.3. Interaction of EM fields and human tissues

To quantify the exposure conditions and the resulting responses for various biological tissues, the specific absorption rate (SAR) is

used. When the EM waves propagate through the tissue, the energy of EM waves is absorbed by the tissue. The SAR is defined as power dissipation rate normalized by material density [31]. The SAR is given by,

$$SAR = \frac{\sigma}{\rho} |E|^2 \quad (5)$$

where E is the electric field intensity (V/m), σ is the electric conductivity (S/m), and ρ is the tissue density (kg/m^3).

3.4. Equations for heat transfer and flow analysis

To solve the thermal problem, a coupled effect of the EM wave propagation and the unsteady bioheat transfer is investigated. The surroundings temperature of the tissue model is fixed at 37 °C except the exposing surface is considered as adiabatic surface. The temperature distribution is corresponded to the SAR. This is because the SAR in the tissue distributes owing to energy absorption. Thereafter, the electromagnetic absorbed energy is converted to thermal energy, which increases the tissue temperature. To reduce the complexity of the problem, the following assumptions are made:

1. The tissue is a bio-material with constant thermal properties.
2. There is no phase change of substance in the tissue.
3. There is local thermal equilibrium between the blood and the tissue.
4. There is no chemical reaction in the tissue.
5. The tissue is assumed to be homogeneous and thermally isotropic and saturated with blood.

This study utilized two pertinent thermal models to investigate the heat transfer behavior of the tissue when exposed to near-field EM radiation.

Model I: The conventional bioheat model

The bioheat model developed by Pennes [4] is one of the earliest models for heat transport in biological tissue. In this model, heat transport in tissues is due to heat conduction, blood perfusion and metabolism. The transient bioheat equation describes effectively how heat transfer occurs within the human tissue, and the equation can be written as

$$\rho C \frac{\partial T}{\partial t} = \nabla \cdot (k \nabla T) + \rho_b C_b \omega_b (T_b - T) + Q_{met} + Q_{ext} \quad (6)$$

where ρ is the tissue density (kg/m^3), C is the heat capacity of tissue (J/kg K), k is thermal conductivity of tissue (W/m K), T is the tissue temperature ($^\circ\text{C}$), T_b is the temperature of blood ($^\circ\text{C}$), ρ_b is the density of blood (kg/m^3), C_b is the heat capacity of blood (J/kg K), ω_b is the blood perfusion rate, Q_{met} is the metabolism heat source (W/m^3) and Q_{ext} is the external heat source (EM heat-source) (W/m^3).

In the analysis, heat conduction between tissue and blood flow is approximated by the blood perfusion term, $\rho_b C_b \omega_b (T_b - T)$.

Model II: The porous media model

The porous media theory for transport in biological tissues is found to be most appropriate since it has fewer assumptions than the conventional bioheat model [14]. In this case, the tissue is modeled as a porous medium and coupled with the Maxwell's equations that describe electromagnetic phenomena in any medium. The Brinkman-extended Darcy model [33] is used to represent the blood flow within the porous tissue. The equations governing flow in a saturated porous medium are given as follows:

Continuity equation:

$$\nabla \cdot \mathbf{u} = 0 \quad (7)$$

Momentum equation:

$$\left(\frac{\rho}{\varepsilon_p} \right) \frac{\partial \mathbf{u}}{\partial t} + \left(\frac{\mu}{\kappa} \right) \mathbf{u} = -\nabla p + \nabla \cdot \left[\left(\frac{1}{\varepsilon_p} \right) \left(\mu (\nabla \mathbf{u} + (\nabla \mathbf{u})^T) \right) \right] + \rho g \beta (T - T_{ref}) \quad (8)$$

where ρ is the tissue density (kg/m^3), β is the volume expansion coefficient ($1/\text{K}$), \mathbf{u} is the velocity (m/s), p is the pressure (N/m^2), μ is the dynamic viscosity (N s/m^2), t is the time, T is the tissue temperature (K), and T_{ref} is the reference temperature considered here, which is 37°C . In the analysis, the porosity (ε_p) used is assumed to be 0.4 and κ is the permeability of a porous tissue (m^2). The effects of buoyancy due to the temperature gradient are modeled using the Boussinesq approximation which states that the density of a given fluid changes slightly with temperature but negligibly with pressure.

The governing equation describing unsteady heat transfer in the tissue is given by:

Energy equation:

$$(\rho C)_{eff} \frac{\partial T}{\partial t} - \nabla \cdot (k_{eff} \nabla T) = -(\rho C)_b \mathbf{u} \cdot \nabla T + Q_{met} + Q_{ext} \quad (9)$$

where

$$(\rho C)_{eff} = (1 - \varepsilon_p)(\rho C)_s + \varepsilon_p(\rho C)_b \quad (10)$$

$$k_{eff} = (1 - \varepsilon_p)k_s + \varepsilon_p k_b \quad (11)$$

are the overall heat capacity per unit volume and overall thermal conductivity, subscripts *eff*, *s* and *b* represent the effective value, solid and blood phase, respectively.

The external heat source term is equal to the resistive heat generated by the EM field (EM power absorbed), which is defined as

$$Q_{ext} = \frac{1}{2} \sigma_{tissue} |\bar{\mathbf{E}}|^2 = \frac{\rho}{2} \cdot \text{SAR} \quad (12)$$

where σ_{tissue} is the electric conductivity of tissue (S/m).

3.4.1. Boundary condition for heat transfer and flow analysis

The heat transfer and flow analysis excluding the surrounding space is considered only in the tissue. The surroundings of the tissue are fixed temperature at 37°C and the boundaries for flow analysis are considered as open boundary where fluid can flow out from the domain or into the domain with a specified exterior temperature.

$$\hat{\mathbf{n}} \cdot \left[-p\mathbf{I} + \left(\frac{1}{\varepsilon_p} \right) \mu (\nabla \cdot \bar{\mathbf{u}} + (\nabla \cdot \bar{\mathbf{u}})^T) \right] = -F_0 \cdot \hat{\mathbf{n}} \quad (13)$$

where $\hat{\mathbf{n}}$ is the normal vector of the boundary, \mathbf{I} is the identity matrix, F_0 is normal stress (N/m^2), μ is the dynamic viscosity ($\text{Pa}\cdot\text{s}$), p is the pressure (Pa), $\bar{\mathbf{u}}$ is the velocity vector (m/s) and ρ is the density (kg/m^3).

The surface where is exposed to EMF is considered as adiabatic and no-slip boundary condition.

$$\hat{\mathbf{n}} \cdot \left[-k_{eff} \nabla T + C_b \bar{\mathbf{u}} T \right] = 0 \quad (14)$$

$$\bar{\mathbf{u}} = 0 \quad (15)$$

The initial temperature is assumed to be uniform throughout the tissue.

$$T(t_0) = 37^\circ\text{C} \quad (16)$$

3.5. Calculation procedure

The coupled model of EM fields propagation, heat transfer and blood flow analysis is solved by FEM. This study provides a variable mesh method for solving the problem as shown in Fig. 3. The system of governing equations as well as the initial and boundary conditions are then solved. All computational processes are implemented using COMSOL™ Multiphysics, to demonstrate the phenomenon that occurs in the tissue exposed to the EM fields.

The 2D model is discretized using triangular elements and the Lagrange quadratic is then used to approximate the temperature and SAR variations across each element. A grid independence test is carried out to identify the suitable number of elements required as shown in Fig. 4. This grid independence test leads to the mesh with approximately 40,000 elements. It is reasonable to assume that, at this element number, the accuracy of the simulation results is independent of the number of elements. The thermal properties and dielectric properties of the tissue and blood used for the calculations are given in Table 1.

4. Results and discussion

This work focuses on the effects of different exposure distances, exposure times, and tissue permeabilities on SAR, blood flow and heat transfer in biological tissue due to EM near-field exposure. The blood convection of the tissue at different exposure conditions induced by EM near-field is systematically investigated. The coupled model equations of the EM propagation and thermal as well as fluid flow are solved numerically.

4.1. Verification of the model

In order to perform verification of the models presented here, the simple case of the simulated results is validated against the numerical results obtained with the same geometric model

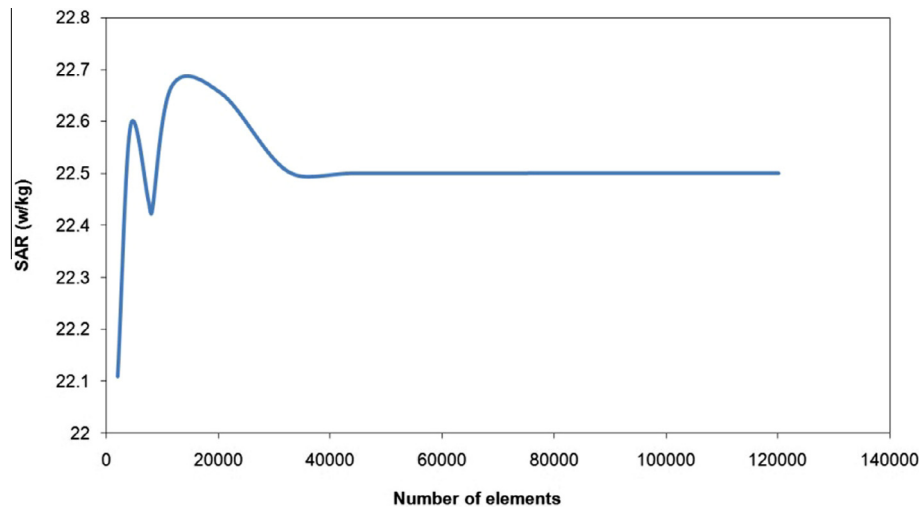


Fig. 4. Grid independence test of the model.

Table 1

Thermal properties and dielectric properties of the tissue.

Tissue properties	Values
Tissue density (ρ)	1000 kg/m ³
Heat capacity of tissue (C)	4000 J/kg K
Heat capacity of blood (C_b)	4000 J/kg K
Thermal conductivity of tissue (k)	0.6 W/m K
Density of blood (ρ_b)	1000 kg/m ³
Blood perfusion rate (ω_b)	0.0001 s ⁻¹
Tissue porosity (ε_p)	0.4
Volume expansion coefficient (β)	1 × 10 ⁻⁴ K ⁻¹
Blood dynamic viscosity (μ)	4 × 10 ⁻³ Pa·s
Relative permittivity (ε_r)	80
Electrical conductivity (σ)	1 S/m

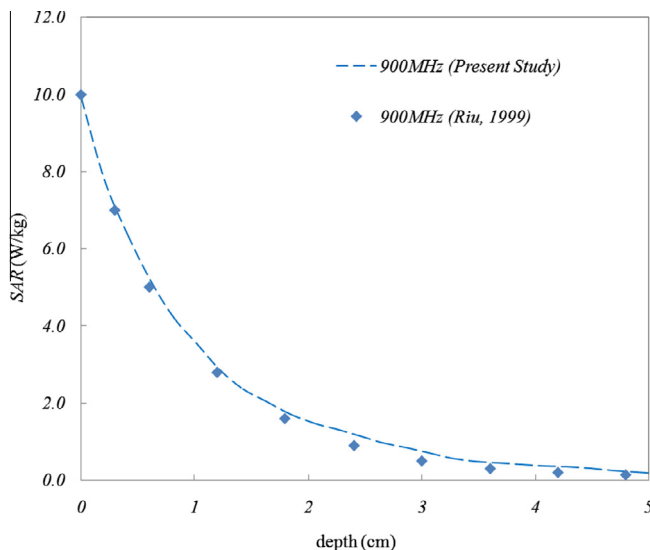


Fig. 5. Comparison of the calculated SAR distribution to the SAR distribution obtained by Riu and Foster [32].

obtained by Riu and Foster [32]. The SAR is determined in a semi-infinite plane of homogeneous tissue model from near-field exposure to a dipole antenna. In the validation case the dipole used operates at 900 MHz frequency and transmits the radiated power of 0.6 W. The result of the validation test case is illustrated in Fig. 5 and clearly shows good agreement of the SAR value of tissue

between the present solution and that of Riu. The SAR decreases exponentially in the wave propagation direction. This favorable comparison lends confidence in the accuracy of the present numerical model and ensures that the numerical model can accurately represent the phenomena occurring at the interaction of EM fields with tissue.

4.2. Effect of exposure distance

In the tissue model, the effect of distance to an EMF source on natural convection in the biological tissue is systematically investigated. The SAR, fluid flow and temperature distributions in the tissue during exposure to EM fields of 900 MHz are obtained by numerical simulation of the EM wave propagation and heat transfer equations. In particular, the results obtained from the porous media model, considered natural convection, are compared with the results obtained from the conventional bioheat model. Fig. 6 shows the SAR distribution evaluated on the tissue model exposed to the near-field EMF at various exposure distances.

The EM absorption pattern in the near-field region typically differs significantly from that occurred at infinity and varies with distance from the source. From Fig. 6 it is found that exposure distance between the dipole antenna and the tissue model significantly influences the distribution shapes of SAR. The SAR distribution pattern and penetration depth of EM energy depend strongly on the distance from the dipole antenna to the tissue. In the tissue closed to the dipole antenna (Fig. 6a), the SAR pattern distributes in a near-circle shape. While for a large distances (Fig. 6d), the SAR pattern being similar to the plane wave exposure. This is because the strong inductive and capacitive effects in the near-field region decrease in SAR very quickly with the distance.

The highest SAR values occur at the surface directly beneath the feed point of the dipole antenna and correspond to the earlier works [32]. The maximum SAR values for the radiated power of 0.6 W are 22.43 W/kg, 8.28 W/kg, 0.84 W/kg, and 0.22 W/kg for the distances of 0.5, 1.0, 3.0, and 5.0 cm, respectively. Comparing to ICNIRP standard for safety level at the maximum SAR value of 2 W/kg (general public exposure) and 10 W/kg (occupational exposure) [1], the obtained SAR values at the exposure distances of 0.5 and 1.0 cm are higher than the ICNIRP exposure limits for general public exposure. (The SAR value depends on dielectric properties of biological tissues; dielectric constant ε_r and electrical conductivity σ).

Since this study has focused on the volumetric heating effect into the tissue induced by near-field EMF, the effect of ambient

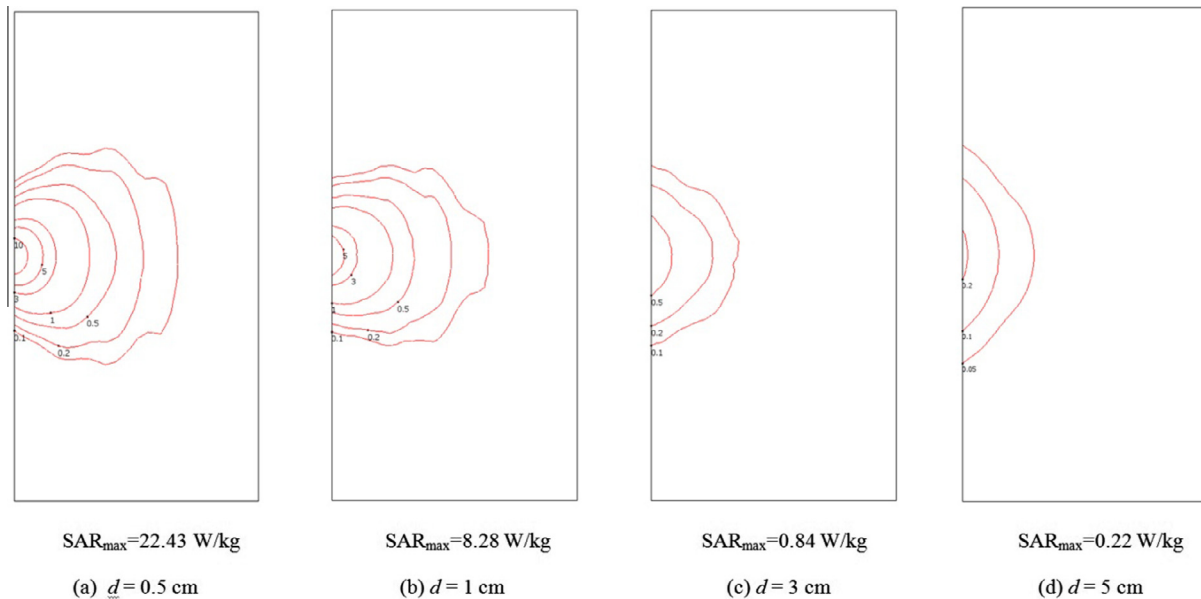


Fig. 6. SAR distribution (W/kg) in the tissue at the exposure distances of (a) 0.5 cm (b) 1 cm (c) 3 cm (d) 5 cm.

convection has been neglected in order to gain insight into the interaction between EM field and tissues as well as the correlation between SAR, heat transfer and fluid flow mechanism. Moreover, the effect of thermoregulation mechanisms has also been neglected due to the small temperature increase occurred during exposure process. The porosity (ϵ_p) used is 0.4 and the permeability of a porous tissue (κ) is assumed to be $5e-7$ m².

In order to study the heat transfer in the tissue, the coupled effects of EM near-field propagation and unsteady heat transfer as well as initial and boundary conditions are then investigated. Due to these coupled effects, the SAR distributions in Fig. 6 are converted into heat by absorption of the tissues.

Fig. 7 shows the temperature distributions and velocity fields in the tissue at various time exposed to the near-field EM frequency of 900 MHz at the radiated power of 0.6 W calculated using the bioheat model (Fig. 7a) and the porous media model (Fig. 7b). For the tissue exposed to the near-field EM for a time, the temperature within the tissue (Fig. 7) is increased corresponding to the SAR (Fig. 6). This is because the absorbed energy is converted to thermal energy, which increases the tissue temperature.

By using the bioheat model, the maximum temperature increases are 0.211 °C, 0.708 °C and 1.092 °C for exposure times of 1 min, 5 min, and 10 min, respectively. By using the porous media model, the maximum temperature increases are 0.211 °C, 0.703 °C and 1.004 °C for exposure times of 1 min, 5 min, and 10 min, respectively (Fig. 6b). The hot spot zone is strongly displayed with semi-sphere shape at 5 min exposure in the area close to the dipole antenna for the both heat transfer models.

In porous media model, the velocity fields vary corresponding to the temperature gradient in the tissue. At 1 min when the convection flow is small, the temperature distribution is mainly governed by conduction heat transfer and there is no apparent temperature difference between the two models. However after 5 min, the maximum temperature increases obtained from the porous media model have a little bit lower temperature than that of the conventional bioheat model. This is due to a dominant effect of blood natural convection in the porous media model, shown in Fig. 7b, plays important roles on the cooling processes in the tissue in a high temperature gradient area. It can be seen that, the maximum temperature increase observed in each case is not much

different; however the observed temperature distribution pattern in each case at a longer period of time is quite different especially in case of 10 min exposure. Moreover the temperature distribution patterns of the porous media model are also distorted by the blood dissipation in natural convection effect, shown in Fig. 7b.

Fig. 8 shows the temperature distributions and velocity fields in the tissue at various exposure distances to a dipole source at the radiated power of 0.6 W calculated using the conventional bioheat model (Fig. 8a) and the porous media model (Fig. 8b). In this case, the tissue is exposed to the near-field EM frequency of 900 MHz for 10 min. Similar to the SAR values, the intensity of the energy absorbed in the vicinity of the antenna is presented. A smaller distance leads to higher electric field intensities, SAR, and heat generation, thereby increasing the temperature within the tissue. The temperature within the tissue shown in Fig. 8 is increased corresponding to the SAR as shown in Fig. 6. It is found that the exposure distance between the dipole antenna and the tissue significantly influences the SAR, velocity field and temperature distribution.

As the exposure distance decreases, the tissue temperature is increased as well. At the large exposure distances of 1, 3, and 5 cm, the SAR values are low compared to those of small exposure distance and the temperature differences between the two models are insignificant. While for the smaller exposure distance of 0.5 cm with higher temperature gradient, the natural convection becomes a dominant effect to dissipate the heat generated by EMF absorption. The temperature increases in porous media model are therefore a little bit lower than that of bioheat model. This is due to the smaller exposure distance leads to higher electric field intensities, SAR, and the intense heat generation induced the convection flow field within the tissue. Moreover the temperature distribution pattern of the porous media model is also distorted by the strong blood dissipation in natural convection effect.

4.3. Effect of permeability of tissue

The biological tissue is divided into the vascular region (blood phase) and the extra-vascular region (tissue phase). Blood flow velocity in the tissue also depends on the permeability of the tissue. The tissue permeability (κ) is naturally related to void ratio,

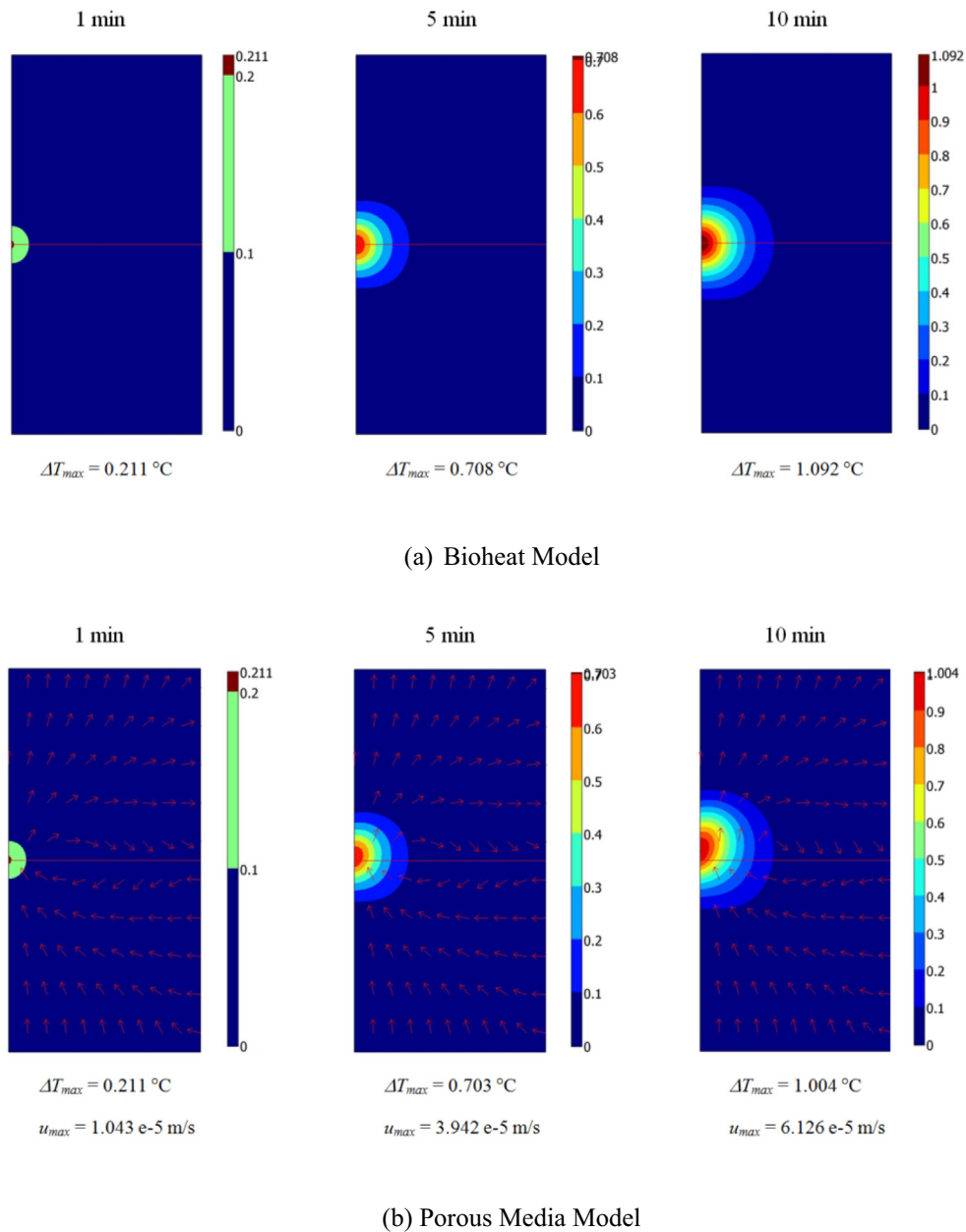


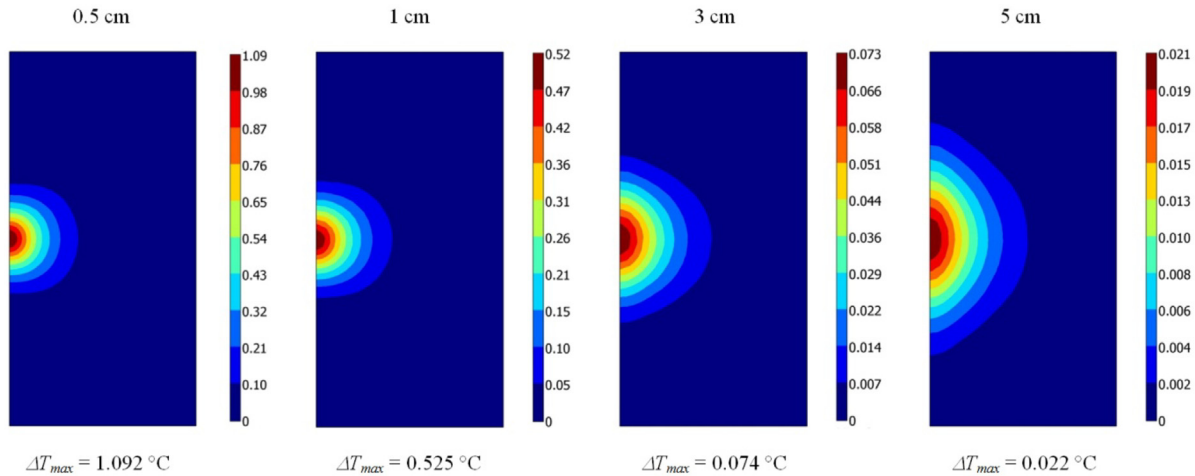
Fig. 7. The temperature and velocity fields in the tissue at various exposure times calculated using (a) the conventional bioheat model (b) the porous model (at $d = 0.5$ cm).

as well as the volumetric fraction of each phase in the porous tissue (saturation). In this study, three different values of permeability, namely, $1e-8$ m², $5e-7$ m², and $1e-6$ m² are used to investigate transport phenomena induced by EM near-field exposure within the tissue.

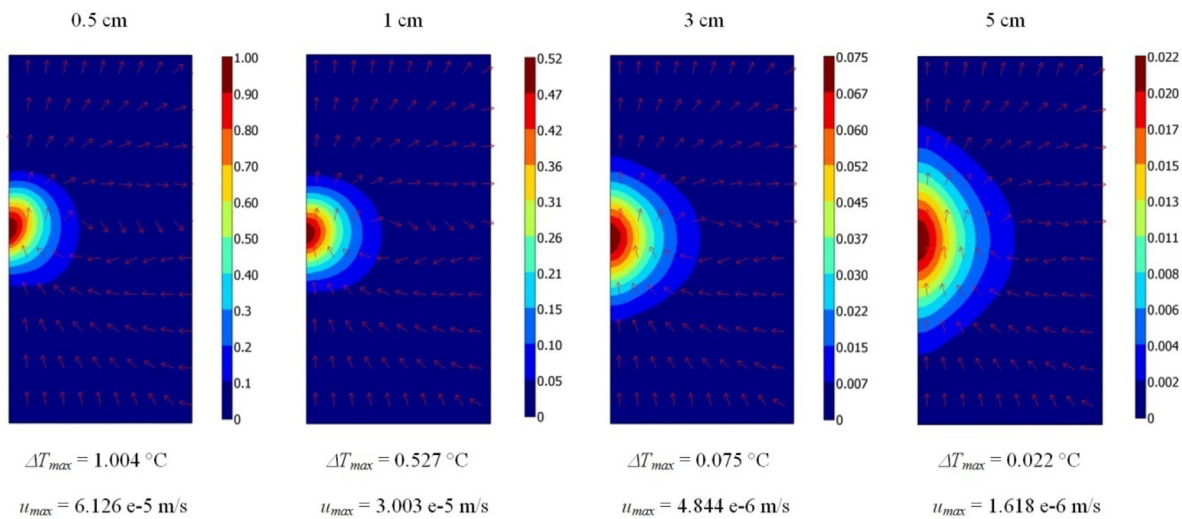
Fig. 9 shows the temperature fields (Fig. 9a) and velocity fields (Fig. 9b) in the tissue with various permeabilities exposure to a 5 W dipole antenna at the distance of 5 cm for 10 min. Comparing the temperature distributions in different tissue permeability values in Fig. 9a, it can be noticed that the peak temperature values of each cases do not exactly occur at the same position. The peak temperature difference of each permeability value is occurred in the vicinity of surface closed to the dipole antenna where blood flows carry energy from the surface into the inner layer of tissue. The maximum temperature increases are 1.552 °C, 1.430 °C and 1.257 °C for the permeability values of $1e-8$ m², $5e-7$ m², and $1e-6$ m², respectively. It is found that the higher permeability

value of the tissue corresponds to the lower temperature increase of tissue. This is because the higher permeability allows greater flow velocity in natural convection due to the low flow resistance of the solid matrix phase. From Fig 9b, it is found that flow velocity in the higher permeability tissue is higher than those in the lower permeability tissues. The fluid velocities are higher close to the exposed surface area since there are higher temperature gradients, thereby leading to a stronger buoyancy-induced flow. For the porous media model, the unsymmetrical temperature field occurred strongly in the higher permeability tissue (Fig. 9a) even though the distribution of EM energy absorbed is symmetry (Fig. 6d). This is due to gravitational effect of the blood flow driven by the near-field EMF.

In the low permeability tissue ($\kappa = 1e-8$ m²), the peak temperature occurred at the same position with regard to the position of the peak SAR value in Fig. 6. This is because in the low permeability tissue, fluid motion is suppressed due to the flow resistance of the



(a) Bioheat Model



(b) Porous Media Model

Fig. 8. The temperature and velocity fields in the tissue at various exposure distances calculated using (a) the conventional bioheat model (b) the porous model (at $t = 10$ min).

porous tissue. Consequently, the fluid is nearly stagnant indicating that conduction is a dominant mode of heat transfer. While in the higher permeability tissue ($5e-7$ m², and $1e-6$ m²) with higher flow velocity, the peak temperature slightly shifted to the higher position (Fig. 9a) corresponds to the flow direction (Fig. 9b). It is concluded that for the tissue subjected to a near-field EMF, the tissue permeability also affects the temperature distribution patterns within the tissue.

5. Conclusions

A numerical analysis of the SAR, fluid flow and heat transfer in the tissue during exposure to a near-field EMF in different exposure conditions has been performed. In the tissue model, the effects of distance to an EMF source and tissue permeability on natural convection in the biological tissue are systematically investigated. The SAR, fluid flow and the temperature distributions in the tissue during exposure to EM fields are obtained by numerical

simulation of EM wave propagation and heat transfer equations. The EM wave propagation is expressed mathematically by Maxwell's equations. The heat transfer model used in this study is developed based on bioheat model and porous media model.

As a result, the SAR distribution pattern and penetration depth of EM energy depend strongly on the distance from the dipole antenna to the tissue. The smaller distance leads to higher electric field intensity, SAR, and heat generation, thereby increasing the temperature within the tissue. As the exposure distance decreases, the tissue temperature is increased as well. The highest SAR values as well as the temperature increases occur at the surface directly beneath the feed point of the dipole antenna.

The results obtained from the porous media model, considered natural convection, are also compared with the results obtained from the conventional bioheat model. By using the different heat transfer models, the distribution patterns of temperature at a particular time are quite different. The maximum temperature increases obtained from the porous media model have a little bit

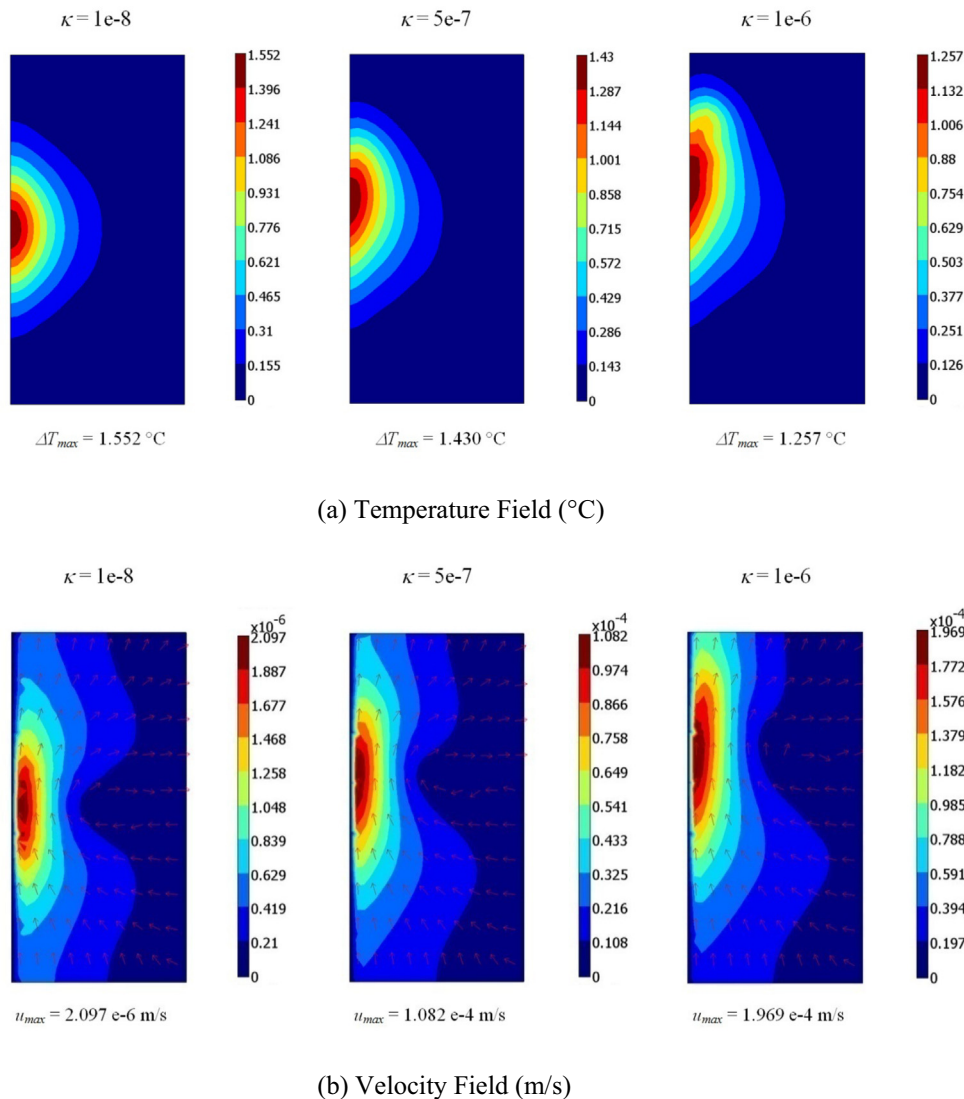


Fig. 9. The temperature and velocity fields of various permeabilities in the tissue exposure to a 5 W dipole antenna at the distance of 5 cm for 10 min.

lower temperature than that of the conventional bioheat model. This is due to a dominant effect of blood natural convection in the porous media model that the velocity fields vary corresponding to the temperature gradient in the tissue.

Moreover, the tissue permeability also affects the temperature distribution patterns within the tissue. The higher permeability value of the tissue corresponds to the lower temperature increase of tissue. The fluid velocities are higher close to the exposed surface area since there are higher temperature gradients, thereby leading to a stronger buoyancy-induced flow. The higher permeability allows greater flow velocity in natural convection due to the low flow resistance of the solid matrix phase. In the low permeability tissue, the fluid flow is retarded by the porous medium structure and the flow is nearly stagnant indicating that conduction is a dominant mode of heat transfer.

The obtained results contribute to the understanding of the realistic situation and prediction of the temperature distribution within the tissue during exposure to the near-field EMFs. This may be of assistance in determining exposure limits for the power output of the wireless transmitter, and its distance from the human body. The results can also be used as a guideline to clinical practitioners in EM relates the interaction of the radiated waves with the human body.

6. Significant of this work

The present study utilizes the porous media theory to analyze SAR, fluid flow and heat transfer in biological tissue subjected to a near-field EMF. The dipole antenna is the most common design for omnidirectional antennas and is used as an EM source in this study. The results obtained from the porous media model, considered natural convection, are also compared with the results obtained from the conventional bioheat model. The obtained results contribute to the understanding of the realistic situation and prediction of the temperature distribution within the tissue during exposure to the near-field EMFs.

Acknowledgments

The authors gratefully acknowledge the Thailand Research Fund (TRF) and Eastern Asia University (under the TRF contract No. TRG5780128).

References

- [1] International Commission on Non-Ionizing Radiation Protection (ICNIRP), Guidelines for limiting exposure to time-varying electric, magnetic and electromagnetic fields (up to 300 GHz), *Health Phys.* 74 (1998) 494–522.

- [2] IEEE, IEEE Standard for Safety Levels with Respect to Human Exposure to Radio Frequency Electromagnetic Fields, 3 kHz to 300 GHz, 1999, IEEE Standard C95.1-1999.
- [3] M.A. Stuchly, Health effects of exposure to electromagnetic fields, in: *Proceedings of the IEEE Aerospace Applications Conference*, vol. 1, 1995, pp. 351–368.
- [4] H.H. Pennes, Analysis of tissue and arterial blood temperature in the resting human forearm, *J. Appl. Physiol.* 1 (1948) 93–122.
- [5] W. Wulff, The energy conservation equation for living tissue, *IEEE Trans. Biomed. Eng.* 21 (6) (1974) 494–495.
- [6] H.G. Klinger, Heat transfer in perfused biological tissue. I: General theory, *Bull. Math. Biol.* 36 (4) (1974) 403–415.
- [7] M.M. Chen, K.R. Holmes, Microvascular contributions in tissue heat transfer, *Ann. N. Y. Acad. Sci.* 335 (1980) 137–150.
- [8] S. Weinbaum, L.M. Jiji, D.E. Lemons, Theory and experiment for the effect of vascular microstructure on surface tissue heat transfer. Part I: Anatomical foundation and model conceptualization, *ASME J. Biomech. Eng.* 106 (4) (1984) 321–330.
- [9] C. Chen, L.X. Xu, A vascular model for heat transfer in an isolated pig kidney during water bath heating, *ASME J. Heat Transfer* 125 (5) (2003) 936–943.
- [10] A. Dhall, A. Halder, A.K. Datta, Multiphase and multicomponent transport with phase change during meat cooking, *J. Food Eng.* 113 (2012) 299–309.
- [11] A.R.A. Khaled, K. Vafai, The role of porous media in modeling flow and heat transfer in biological tissues, *Int. J. Heat Mass Transfer* 46 (2003) 4989–5003.
- [12] K. Khanafer, K. Vafai, Transport through porous media – a synthesis of the state of the art for the past couple of decades, *Ann. Rev. Heat Transfer* 14 (2005) 345–383.
- [13] K. Khanafer, K. Vafai, The role of porous media in biomedical engineering as related to magnetic resonance imaging and drug delivery, *Heat Mass Transfer* 42 (2006) 939–953.
- [14] A.R. Khaled, K. Vafai, The role of porous media in modeling flow and heat transfer in biological tissues, *Int. J. Heat Mass Transfer* 46 (2003) 4989–5003.
- [15] A. Nakayama, F. Kuwahara, A general bioheat transfer model based on the theory of porous media, *Int. J. Heat Mass Transfer* 51 (11–12) (2008) 2637–3256.
- [16] K. Khanafer, K. Vafai, Synthesis of mathematical models representing bioheat transport, in: W.J. Minkowycz, E.M. Sparrow (Eds.), *Advance in Numerical Heat Transfer*, vol. 3, Taylor & Francis, 2009.
- [17] K. Wang, F. Tavakkoli, S. Wang, K. Vafai, Analysis and analytical characterization of bioheat transfer during radiofrequency ablation, *J. Biomech.* 48 (2015) 930–940.
- [18] M. Iasiello, K. Vafai, A. Andreozzi, N. Bianco, F. Tavakkoli, Effects of external and internal hyperthermia on LDL transport and accumulation within an arterial wall in the presence of a stenosis, *Ann. Biomed. Eng.* 43 (2015) 1585–1599.
- [19] T. Wessapan, S. Srisawatdhisukul, P. Rattanadecho, Numerical analysis of specific absorption rate and heat transfer in the human body exposed to leakage electromagnetic field at 915 MHz and 2450 MHz, *ASME J. Heat Transfer* 133 (2011) 051101.
- [20] T. Wessapan, S. Srisawatdhisukul, P. Rattanadecho, The effects of dielectric shield on specific absorption rate and heat transfer in the human body exposed to leakage microwave energy, *Int. Commun. Heat Mass Transfer* 38 (2011) 255–262.
- [21] T. Wessapan, P. Rattanadecho, Numerical analysis of specific absorption rate and heat transfer in human head subjected to mobile phone radiation, *ASME J. Heat Transfer* 134 (2012) 121101.
- [22] T. Wessapan, S. Srisawatdhisukul, P. Rattanadecho, Specific absorption rate and temperature distributions in human head subjected to mobile phone radiation at different frequencies, *Int. J. Heat Mass Transfer* 55 (2012) 347–359.
- [23] T. Wessapan, P. Rattanadecho, Specific absorption rate and temperature increase in human eye subjected to electromagnetic fields at 900 MHz, *ASME J. Heat Transfer* 134 (2012) 091101.
- [24] T. Wessapan, P. Rattanadecho, Specific absorption rate and temperature increase in the human eye due to electromagnetic fields exposure at different frequencies, *Int. J. Heat Mass Transfer* 64 (2013) 426–435.
- [25] T. Wessapan, P. Rattanadecho, Influence of ambient temperature on heat transfer in the human eye during exposure to electromagnetic fields at 900 MHz, *Int. J. Heat Mass Transfer* 70 (2014) 378–388.
- [26] T. Wessapan, P. Rattanadecho, Heat transfer analysis of the human eye during exposure to sauna therapy, *Numer. Heat Transfer, Part A: Appl.* 68 (2015) 566–582.
- [27] P. Keangin, T. Wessapan, P. Rattanadecho, Analysis of heat transfer in deformed liver cancer modeling treated using a microwave coaxial antenna, *Appl. Therm. Eng.* 31 (16) (2011) 3243–3254.
- [28] P. Keangin, T. Wessapan, P. Rattanadecho, An analysis of heat transfer in liver tissue during microwave ablation using single and double slot antenna, *Int. Commun. Heat Mass Transfer* 38 (2011) 757–766.
- [29] P. Rattanadecho, P. Keangin, Numerical study of heat transfer and blood flow in two-layered porous liver tissue during microwave ablation process using single and double slot antenna, *Int. J. Heat Mass Transfer* 58 (2013) 457–470.
- [30] P. Keangin, K. Vafai, P. Rattanadecho, Electromagnetic field effects on biological materials, *Int. J. Heat Mass Transfer* 65 (2013) 389–399.
- [31] E.R. Adair, B.W. Adams, G.M. Akel, Minimal changes in hypothalamic temperature accompany microwave-induced alteration of thermoregulatory behavior, *Bioelectromagnetics* 5 (1984) 13–30.
- [32] P.J. Riu, K.R. Foster, Heating of tissue by near-field exposure to a dipole, *IEEE Trans. Biomed. Eng.* 46 (8) (1999) 911–917.
- [33] H.C. Brinkman, A calculation of the viscous force exerted by a flowing fluid on a dense swarm of particles, *Appl. Sci. Res. A1* (1949) 27–34.